Supplementary Information

Ultrathin Nanosheets of Aluminosilicate FER Zeolite Synthesized in the Presence of a Sole Small Organic Ammonium

Hao Xu,‡[a] Wei Chen,‡[b] Guanqun Zhang,[c] Pengfei Wei,[d] Qinming Wu,*[,a] Longfeng Zhu,[e] Xiangju Meng,[a] Xiujie Li,[d] Jinhua Fei,[a] Shichao Han,[a] Qiuyan Zhu,[a] Anmin Zheng,[b,f] Yanhang Ma,*[,c] and Feng-Shou Xiao*[,a]

[a]Key Laboratory of Applied Chemistry of Zhejiang Province, Zhejiang University, Hangzhou 310028, China

[b]State Key Laboratory of Magnetic Resonance and Atomic and Molecular Physics, Wuhan Center for Magnetic Resonance, Wuhan Institute of Physics and Mathematics, Wuhan 430071, China

[c]School of Physical Science and Technology, ShanghaiTech University, Shanghai 201210, China

[d]State Key Laboratory of Catalysis, Dalian Institute of Chemical Physics, Dalian 116023, China

[e]College of Biological, Chemical Sciences and Engineering, Jiaxing University, Jiaxing 314001, China

[f]School of Materials Science and Engineering, Zhengzhou University, Zhengzhou, Henan 450052, P. R. China

‡These authors contributed equally to this work.

*E-mail: qinmingwu@zju.edu.cn; mayh2@shanghaitech.edu.cn; fsxiao@zju.edu.cn

Experimental

Computational Method

All DFT calculations in this study were employed by DMol^3 software, and the exchange-correlation energy was described by the PBE functional with Grimme's dispersion correction (DFT-D3). The Brillouin-zone sampling was restricted to the Γ point. The DND basis set with all electron treatment was used, and the convergence criterion for the electronic self-consistency cycle was set as 10^{-5} ***a.u.*** The convergence criterions of optimization for energy difference, maximum force, and maximum displacement were set as 2×10^{-5} ***a.u.***, 0.004 ***a.u.***/Å, and 0.005 Å, respectively.

The pure silicon model was used in all calculations to avoid the complicate discussions referred to Al distribution, and the nitrogen atom in OSDA molecule was replaced by carbon atom to neutralize the positive charge, and all system keeps neutral. These approximations will simplify uncertain factors but keep the key factor, *i.e.*, the geometry characters of OSDA and slab, and it's also reasonable because the nitrogen atom in OSDA was surrounded by four carbon atoms, which is hard to strongly interact with the atoms in slab. Moreover, the neutral system would help to improve the accuracy of energy calculation and avoid the influence from additional charges of OSDA.

To calculate the surface energy and adsorption energy of different number OSDA on FER {100} surface, the surface was cleaved from 1×1×2 supercell to contain more OSDA molecules, and the vacuum gap in the slab is kept large enough (~50 Å) to prevent unphysical interaction between the top and the bottom of the surface or OSDA. To reduce the calculation cost of surface energy calculation on different thickness slab, the FER {100} surface was re-cleaved from unit cell of FER bulk structure. The OSDA adsorption energy on FER {100} surface can reach the maximum where is four OSDAs on FER {100} surface, therefore, the optimal number of OSDA adsorbed on FER {100} surface based on ***p***×1×1 cell of FER bulk structure should be two (***p*** is the layer of FER {100}), and then different thickness slabs from ***p***=1 to ***p***=6 with two OSDA molecules were used to calculate the surface energy.

The adsorption energy (ΔE) is defined as: $\Delta E= E_{slab\_nOSDA}-E_{slab}-E_{nOSDA}$

The surface energy (γ) is defined as: $\gamma=(E_{slab\_nOSDA}-\boldsymbol{p}E_{bulk}-\boldsymbol{m}E_{water}-\boldsymbol{n}E_{OSDA})/2A$

where A is the surface area of FER {100} surface, E_{slab_nOSDA}, E_{slab}, E_{bulk}, E_{water}, and E_{OSDA} are the energy of slab structure adsorbed ***n*** OSDA molecules, slab structure, bulk structure (unit cell), water, and OSDA, ***p*** is number of supercell used for slab structures, ***m*** and ***n*** are the number of water molecules added to terminate the slab structure and OSDA adsorbed on surface.

Note that the variation tendency of surface energy with the number of layers is a para-curve. Normally, the interaction between FER slab and OSDA would increase with the increasing of thickness of slab and reach the platform finally, but the surface energy reaches the minimum at ***p***=3 because the present thickness is the best balance of effect between surface hydroxy and OSDA, which explains the lowest thickness on experiment. Certainly, It can be anticipated that the surface energy would become to reach platform when ***p***$\geqslant$7, but this large amount of atoms in slab ($\geqslant$762 atoms) are hard to be handled by density functional theory.

Materials

Sodium metaaluminate ($NaAlO_2$, AR, 99%, Sinopharm Chemical Reagent Co., Ltd.), sodium hydroxide (NaOH, AR, 96%, Sinopharm Chemical Reagent Co., Ltd.), colloidal silica (40 wt% SiO_2 in water, Sigma-Aldrich Reagent Co., Ltd.), *cis*-2,6-dimethylpiperidine (Sigma-Aldrich Reagent Co., Ltd.), potassium bicarbonate ($KHCO_3$, AR, 99.5%, Sinopharm Chemical Reagent Co., Ltd.), iodoethane (99%, Aladdin Chemical Co., Ltd.), methanol (Sinopharm Chemical Reagent Co., Ltd.), trichloromethane (AR, 99%, Sinopharm Chemical Reagent Co., Ltd.), diethyl ether (AR, 99.5%, Sinopharm Chemical Reagent Co., Ltd.), anion-exchange resin (Amberlite IRN-78, OH-form, Thermofisher Chemical Reagent Co., Ltd.), and ammonium nitrate (NH_4NO_3, AR, 99%, Beijing Chemical Reagent Co., Ltd.) were used without further purification. The deionized water was home-made.

Synthesis

Synthesis of organic template

In the process of synthesis of N,N-diethyl-*cis*-2,6-dimethylpiperidine iodide, a certain amount of *cis*-2,6-dimethylpiperidine and iodoethane were dissolved into methanol, then an excess of $KHCO_3$ was added. The mixture was refluxed at 70 °C for 96 h. After that, the solid product was obtained by filtrating and washing with trichloromethane and diethyl ether. Hydroxide form (denoted as DMPOH) of the product was obtained from anion-exchange with resin.

Synthesis of conventional FER zeolite sample

In a typical run for synthesizing conventional FER zeolite, 0.165 g of $NaAlO_2$, 0.20 g of NaOH, 15.35 g of deionized water, and 2.95 g of 40% colloidal silica solution were mixed and stirred for 2 h. Then 0.05 g of FER seeds was added. After stirring for 10 min, the mixture was transferred to an autoclave and sealed. After heating at 140 °C for 48 h, the sample (C-FER) was obtained by filtrating, washing, and drying. The H-form of the sample (denoted as H-C-FER) was prepared by ion-exchange with NH_4NO_3 solution and calcination at 550 °C for 4 h. The ion-exchange procedure was repeated once.

Synthesis of ultrathin nanosheets of FER zeolite

In a typical run for synthesizing ultrathin nanosheets of FER zeolite, 0.165 g of $NaAlO_2$ was dissolved into 6.5 g of deionized water. Then, 10 g of DMPOH solution (0.23 M in water), 0.254 g of NaOH, and 2.95 g of 40% colloidal silica solution were added. After stirring for 2 h, the mixture was transferred to an autoclave and sealed. After heating at 140 °C for 48 h, the sample denoted as N-FER was obtained from filtrating, washing, and drying at room temperature. The removal of organic templates in the as-synthesized zeolites was calcination at 550 °C for 4 h. The H-form of the N-FER (denoted as H-N-FER) was prepared by ion-exchange with NH_4NO_3 solution and calcination at 550 °C for 4 h. The ion-exchange procedure was repeated once.

Characterizations

X-ray powder diffraction (XRD) patterns were measured with a Rigaku Ultimate VI X-ray diffractometer (40 kV, 40 mA) using CuKα (λ=1.5418 Å) radiation. Scanning electron microscope (SEM) experiments were carried out on JEOL JSM-7800 Prime and Hitachi SU-8010 electron microscopes. The N_2 sorption isotherms at the temperature of liquid nitrogen were measured using Micromeritics ASAP 2020M and Tristar system. Transmission electron microscopy (TEM) experiments were performed on a JEM-2100Plus at 200 kV (Cs = 1.0 mm). The sample composition was determined by inductively coupled plasma (ICP) with a Perkin-Elmer 3300DV emission spectrometer. ^{29}Si and ^{27}Al MAS NMR spectra were recorded on a Varian Infinity Plus 400 spectrometer. ^{13}C NMR experiments were performed on a Bruker Avance-500 spectrometer. The thermogravimetry-differential thermal analysis (TG-DTA) experiments were carried out on a Perkin-Elmer TGA 7 unit in air at heating rate of 10 °C/min in the temperature range from room temperature to 800 °C. The acidity of the catalysts was measured by the temperature-programmed-desorption of ammonia (NH_3-TPD). 140 mg of the samples were placed in a quartz tube and pretreated in He flow at 600 °C for 30 min. Then the temperature was reduced to 150 °C. NH_3 passed through the samples until reach equilibrium for 30 min. When the baseline was stable, the signal of NH_3 desorption was monitored by the thermal conductivity detector (TCD) in He flow at a heating rate of 20 °C /min from 150 to 600 °C. The acid concentrations of Brönsted and Lewis acid sites of the samples were investigated by exploring pyridine adsorption in a Bruker VERTEX70 FTIR soectroscopy. The sample was pretreated at 450 °C under vacuum for 1 h. After cooling to 30 °C, the background was scanned. Adsorption of pyridine was performed at 300 °C for 15 min. The cell was vacuumed at 150 °C for 30 min and scanned after cooled to 30 °C.

Catalytic tests

The skeletal isomerization reaction of 1-butene to isobutene was carried out in a fixed bed micro-reactor with an inner diameter of 7 mm under atmospheric pressure. At first, 0.5 g of the catalyst (20-40 mesh, H-FER zeolite) was activated at 500 °C in N_2 flow for 2 h. After the temperature was cooled to 400 °C, the mixture flow of 1-butene with nitrogen (1:1) was fed into the fixed bed with the weight hourly space velocity (WHSV) of 8 h^{-1}. The reaction products were analyzed online by an Agilent 7890B gas chromatograph equipped with a flame ionization detector (FID) and an Al_2O_3 capillary column.

Supplementary Figure Captions

Figure S1. Powder XRD pattern of the as-synthesized ultrathin nanosheets of FER zeolite (N-FER).

Figure S2. Powder XRD pattern of the as-synthesized conventional FER zeolite (C-FER).

Figure S3. SEM images of the as-synthesized C-FER with various scale bars.

Figure S4. Powder XRD pattern of the H-N-FER zeolite.

Figure S5. Powder XRD pattern of the H-C-FER zeolite.

Figure S6. N_2 sorption isotherms of the (a) H-N-FER and (b) H-C-FER.

Figure S7. ^{29}Si MAS NMR spectrum of the as-synthesized N-FER.

Figure S8. ^{27}Al MAS NMR spectrum of the as-synthesized N-FER.

Figure S9. ^{13}C NMR spectra of the (a) as-synthesized N-FER dissolved in HF solution and (b) DMPOH solution.

Figure S10. TG-DTA curves of the as-synthesized N-FER.

Figure S11. SEM images of N-FER samples crystallized for 24-40 h.

Figure S12. TEM image of N-FER samples crystallized for 32 h.

Figure S13. NH_3-TPD profiles of the (a) H-N-FER and (b) H-C-FER.

Figure S14. Pyridine-IR spectra of the (a) H-N-FER and (b) H-C-FER.

Table S1. Textural parameters of the H-N-FER and H-C-FER.

Table S2. EDS analysis of the C-FER and N-FER samples during crystallization process.

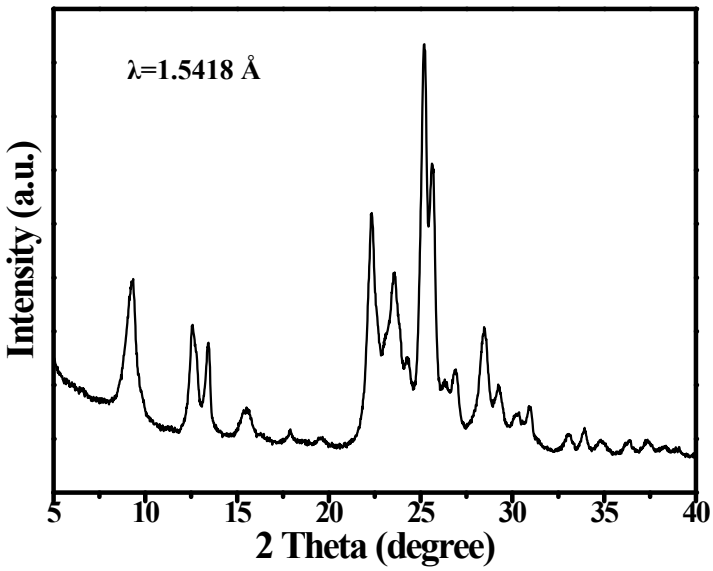

Figure S1. Powder XRD pattern of the as-synthesized ultrathin nanosheets of FER zeolite (N-FER).

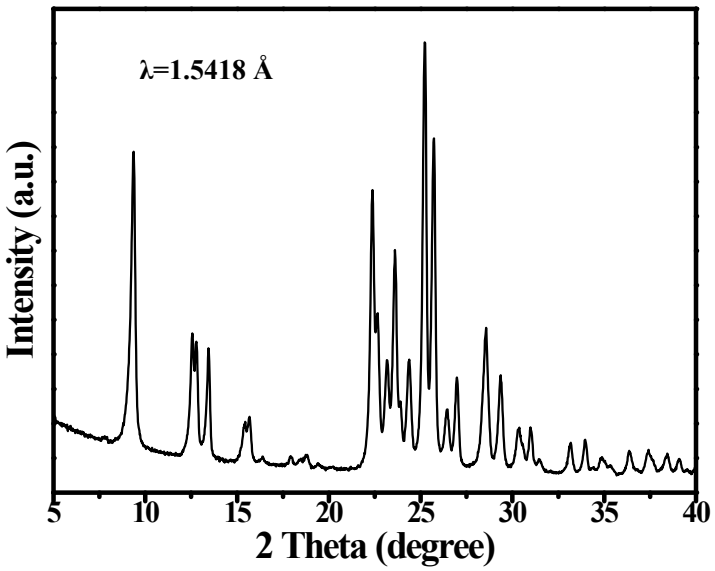

Figure S2. Powder XRD pattern of the as-synthesized conventional FER zeolite (C-FER).

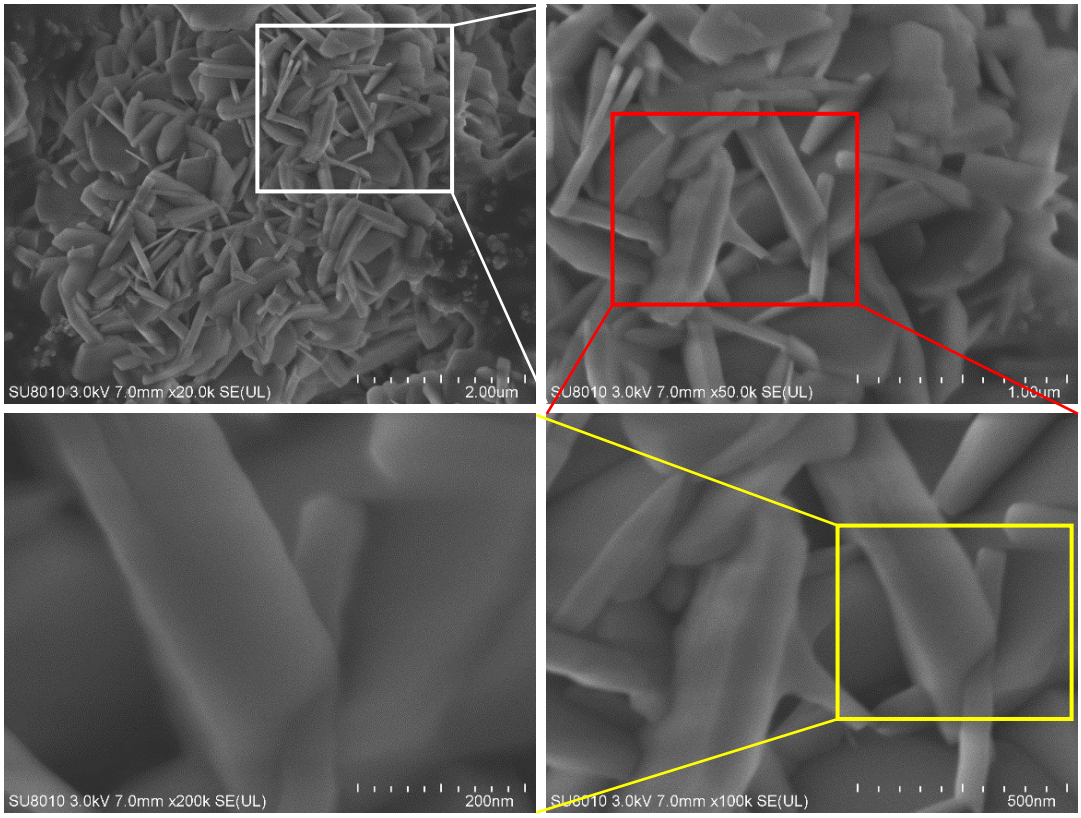

Figure S3. SEM images of the as-synthesized C-FER with various scale bars.

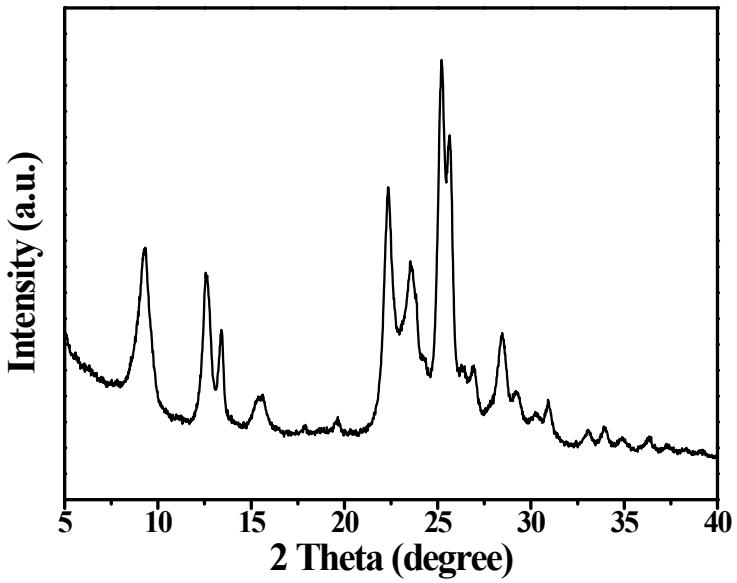

Figure S4. Powder XRD pattern of the H-N-FER zeolite.

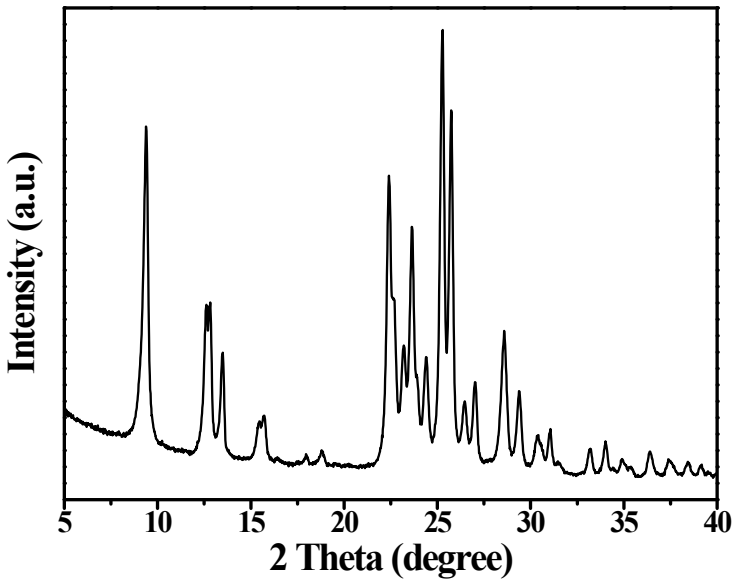

Figure S5. Powder XRD pattern of the H-C-FER zeolite.

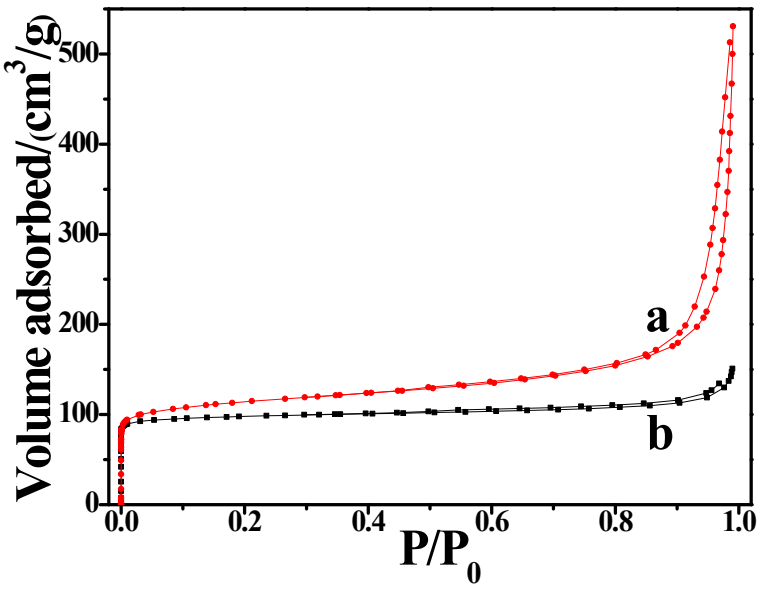

Figure S6. N_2 sorption isotherms of the (a) H-N-FER and (b) H-C-FER.

Note: H-N-FER and H-C-FER give the BET surface areas of 391 m^2/g and 326 m^2/g and the micropore volume of 0.14 and 0.14 cm^3/g.

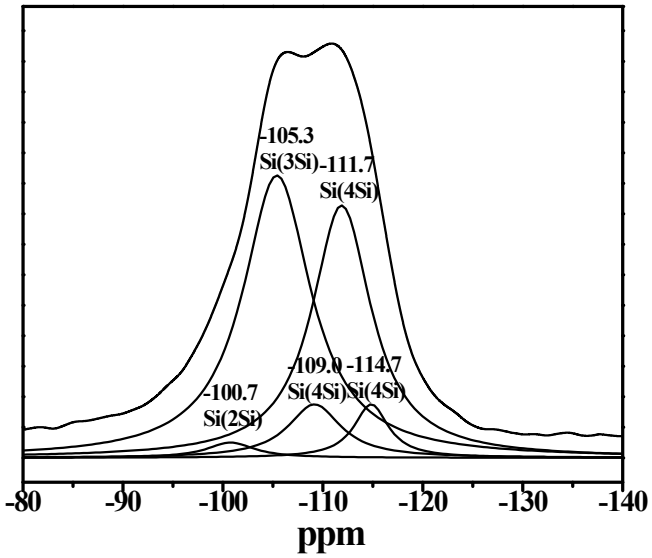

Figure S7. ^{29}Si MAS NMR spectrum of the as-synthesized N-FER.

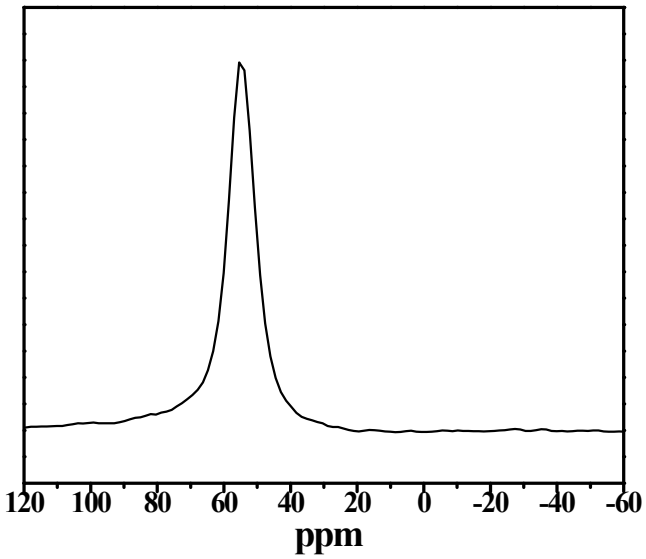

Figure S8. ^{27}Al MAS NMR spectrum of the as-synthesized N-FER.

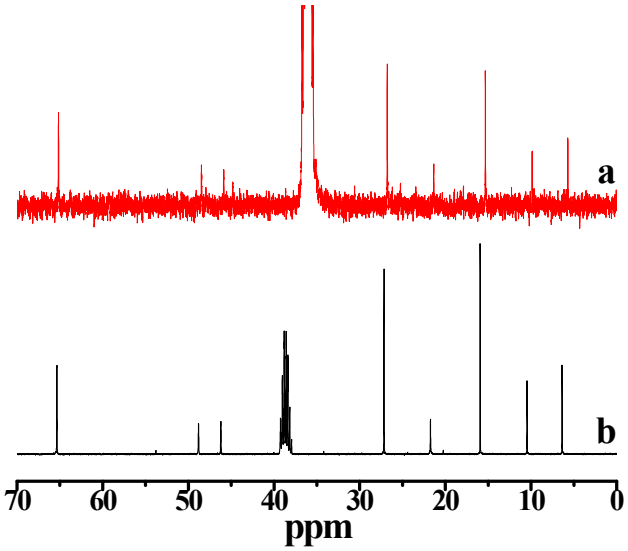

Figure S9. ^{13}C NMR spectra of the (a) as-synthesized N-FER dissolved in HF solution and (b) DMPOH solution.

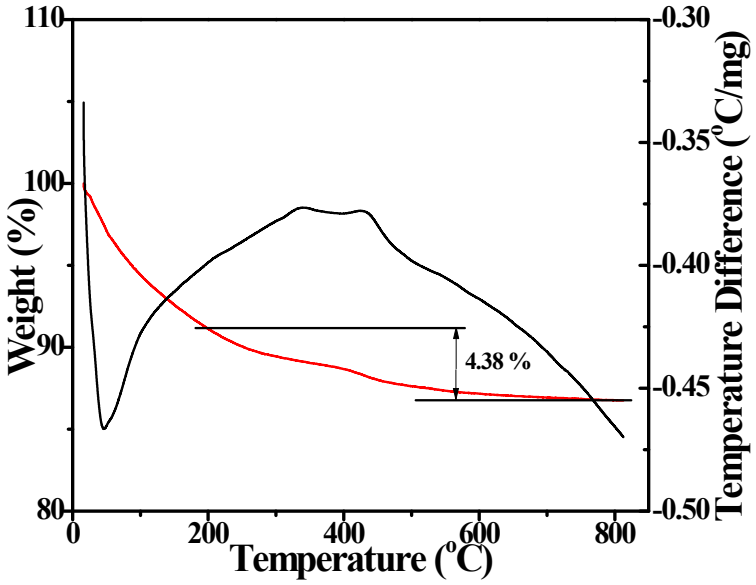

Figure S10. TG-DTA curves of the as-synthesized N-FER.

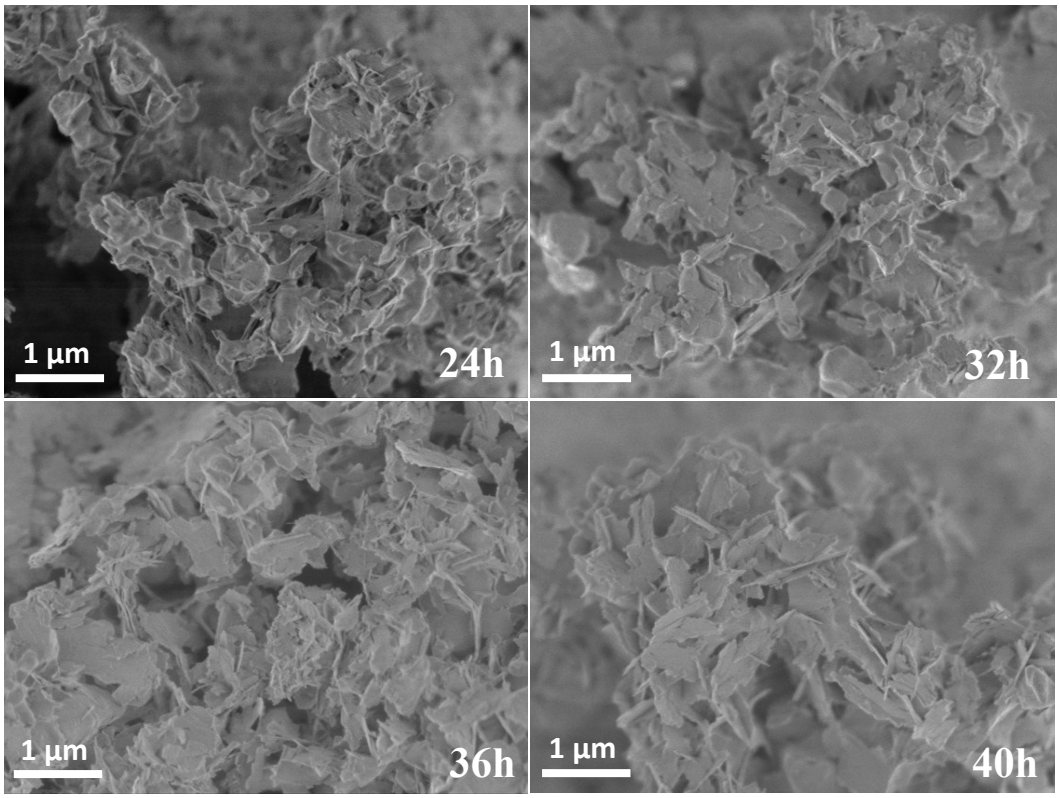

Figure S11. SEM images of N-FER samples crystallized for 24-40 h.

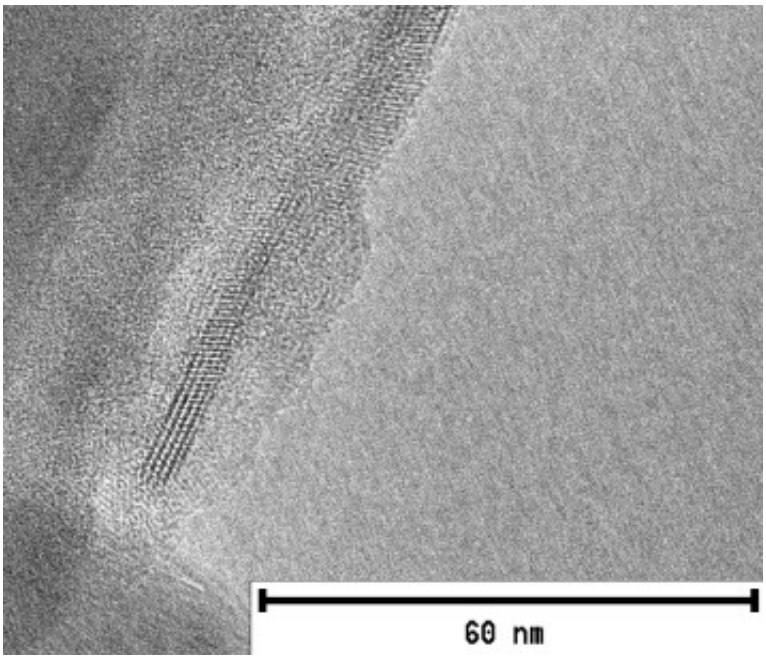

Figure S12. TEM image of N-FER samples crystallized for 32 h.

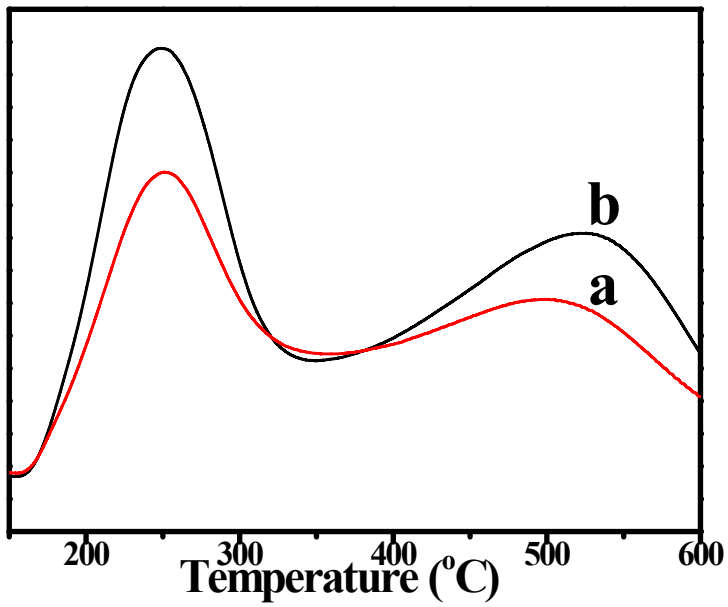

Figure S13. NH_3-TPD profiles of the (a) H-N-FER and (b) H-C-FER.

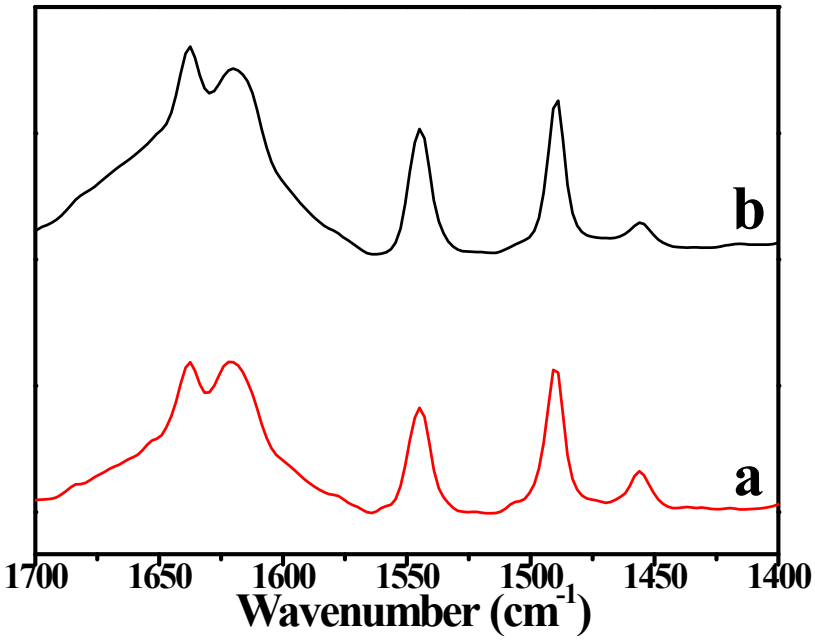

Figure S14. Pyridine-IR spectra of the (a) H-N-FER and (b) H-C-FER.

Table S1. Textural parameters of the H-N-FER and H-C-FER.

sample	S_{BET} (m^2/g)	S_{micro} (m^2/g)	S_{ext} (m^2/g)	V_{tot} (cm^3/g)	V_{micro} (cm^3/g)	V_{meso} (cm^3/g)	Si / Al (by ICP)
H-N-FER	391	286	105	0.79	0.14	0.65	8.0
H-C-FER	326	303	23	0.23	0.14	0.09	8.5

Table S2. EDS analysis of the C-FER and N-FER samples during crystallization process.

sample	Al/Si ratio	Na/Si ratio	Na/Al ratio
C-FER	0.12	0.12	0.96
N-FER-24h	0.17	0.14	0.83
N-FER-32h	0.13	0.08	0.56
N-FER-36h	0.14	0.07	0.51
N-FER-40h	0.14	0.05	0.36